ICAS 2016
30th Congress of the International Council of the Aeronautical Sciences
DCC, Daejeon, Korea : September 25-30, 2016

CHAOS THEORY APPLIED TO BUCKLING ANALYSIS OF COMPOSITE CYLINDRICAL SHELL

M. Alfano* and C. Bisagni**
***Department of Aerospace Science and Technology, Politecnico di Milano, Milan, Italy, michela.alfano@polimi.it**
****Faculty of Aerospace Engineering, Delft University of Technology, Delft, Netherlands, c.bisagni@tudelft.nl**

Keywords: *Buckling, Chaos Theory, Sandwich Composite Shells, Cut-outs.*

Abstract

The present paper proposes a chaos approach for the buckling analysis of cylindrical shells under axial compression. The approach is developed using concepts of chaos theory, and is applied to investigate the buckling behavior of sandwich composite shells that are imperfection-sensitivity structures. Two shell configurations are here analyzed, one of them with cut-outs. The goal of the approach is to obtain an erosion profile as function of the increasing axial load, that through a graphical visualization allows to illustrating concisely the effect of geometric imperfections on the load-carrying capability of the shells.
The paper presents an innovative use of the concepts of chaos. The approach can be adopted when an experimental database of imperfections is rarely available to achieve a first assessment of the imperfection sensitivity of axially-compressed shells.

1. Introduction

The buckling response of cylindrical shells under axial compression is affected by the manufacturing and in-service imperfections, which are recognized to be the primary sources of the wide discrepancy between theoretical and experimental results [1]. Currently, shell design relies on NASA SP-8007 guideline [2], which recommends the use of an empirical knockdown factor to account for the influence of imperfections. However, the aerospace industry demands for improved shell design criteria that enable for a reduction of developing and operating costs and, if possible, for lighter structures. Several studies were published in the last years regarding experimental and numerical investigations of the influence of the initial imperfections on the buckling of composite cylindrical shells [3-7].

The use of concepts of the chaos in buckling investigation of axially-compressed shells has been discussed in literature over the last years. The chaos theory [8] concerns non-linear dynamic systems that exhibit seemingly-unpredictable behavior. Actually, it is governed by an underlying order and by a high sensitivity to input conditions. Due to the high imperfections-sensitivity, the buckling behavior of the cylindrical shells can be considered chaotic. Moreover, the transition from pre-buckling equilibrium state to post-buckling equilibrium state is a dynamic process that induces nonlinearities.

El Naschie [9] showed the development of the "spatial chaos" in buckled isotropic cylindrical shells, referring with this term to the development of spatially-chaotic deformation patterns, which are independent on the time and can be perturbed by geometric imperfections.

The dynamic buckling, which deals with the study of the shells under the action of oscillation loads and pulse loads, was studied in terms of temporal chaos by few authors [10-11]. It was observed that small changes in the initial conditions lead to vastly different solutions of the system response over the time. Gonçalves et al. [10] proposed to measure the integrity of the structural response of axially-compressed shells by analyzing the evolution of the basins of attraction of the stable operating points as a

function of the input parameters. An attractor is surrounded in phase space by its own basin of attraction, which defines an ensemble of initial conditions leading towards a common attracting response. The authors investigated both the static and dynamic buckling response of shells and concluded that the safe basin of attraction shrinks as the axial load approaches the buckling load and it is also affected by the initial conditions.

The concept of safe basin was first introduced by Thompson et al. [12]. They argued that the safety of a structure depends not only on the stability of the obtained solutions, but also on the safe basins of attraction surrounding the solutions. The basin can be eroded as the system parameters change. To evaluate the erosion of the safe basin, Soliman and Thompson [13] and Rega and Lenci [14] proposed three measures of integrity. The erosion profile is traced by plotting the integrity measure in function of the varying system parameters, and they show how the integrity measures enable to study the safety of a structure with changing system parameters.

The present paper addresses the application of concepts of the chaos theory to the buckling of cylindrical shells under axial compression. A chaos approach is developed to investigate the influence of geometric imperfections on the safe basin which surrounds the equilibrium configuration related to the buckling load of nominally-perfect shells. In particular, the approach aims to illustrate, through the definition of an erosion profile, the shrinkage of the safe basin in favor of the unsafe basin with the increase in axial compression.

The developed approach is then applied to study the buckling of two composite sandwich shells, one of them with three circular cut-outs.

The approach can be applied to study laminated composite shells and sandwich composite shells in a preliminary design phase when a test-originated database of imperfections is rarely available, and can help to achieve a first assessment of the shell imperfection-sensitivity.

2. Description of the Shells

The two shell configurations here analyzed are scaled models of the Dual Launch System (SYLDA) of Ariane 5 launcher. The shells were previously studied in the European project DESICOS [15-16].

They have an average radius and a free length equal to 350 *mm* and 620 *mm*, respectively. They are made of a sandwich consisting of two composite facesheets and a core.

The inner and outer facesheets are three-ply composite laminates. Each ply is 0.131 *mm* thick and has the material properties listed in Table 1.

Property	**Value**
Longitudinal modulus, E_{11}	150000 MPa
Transverse modulus, E_{22}	9080 MPa
Shear modulus, G_{12}	5290 MPa
Poisson's ratio, ν_{12}	0.32
Density, ρ	1570 kg/m^3

Table 1. Hexcel IM7/8552 UD carbon prepreg [17].

The core of the sandwich is foam with thickness of 1.5 *mm*, whose material properties are reported in Table 2.

Property	**Value**
Young modulus of core, E	350 MPa
Shear modulus, G	150 MPa
Poisson's ratio, ν	0.33
Density, ρ	205 kg/m^3

Table 2. EVONIK Rohacell WF200 [18].

The layup of the shell is [19°/-19°/90°/CORE/90°/-19°/19°], for a total thickness equal to 2.286 *mm*.

The first configuration (named SYLDA) does not have cut-outs, whereas the second one (named SYLDA with cut-outs) includes the presence of three circular cut-outs. A cut-out of diameter equal to 92 *mm* is located on one side of the shell and two smaller cut-outs of diameter equal to 46 *mm* on the other side. The centers of the two smaller cut-outs have a distance of 92 *mm*.

3. Finite Element Model

The finite element models of the shells are realized in ABAQUS v.6.13 [19], using S4R shell elements.

They are shown in Fig. 1, together with the details of the mesh around the cut-outs. The mesh size is 10 *mm* x 10 *mm*, whereas the elements around the larger cut-out and around the two smaller cut-outs have size equal to 4 *mm* x 4 *mm* and 3.6 *mm* x 3.6 *mm*, respectively.

The shell model is fixed at the one end, while all degrees of freedom except the axial translation are constrained at the loaded edge.

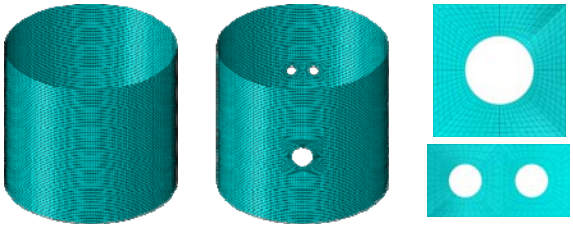

SYLDA SYLDA with cut-outs

Fig. 1. Finite element models of sandwich shells.

4. Chaos Approach

Concepts of the chaos theory are exploited to develop a chaos approach with the aim to investigate the robustness of the fundamental equilibrium state of the cylindrical shells against perturbations given by input imperfections.

A performance function describing the load-carrying capability of shells is assessed over a control domain, which is defined in terms of perturbations of the control parameters used in modeling the input imperfections. For each increment in applied axial load, the safe basin which surrounds the equilibrium state corresponding to the buckling load of nominally-perfect shells may be identified over the control domain. The extension of the safe basin shrinks as axial compression increases. As a consequence, the load-carrying capability of the shells falls off.

To estimate the degradation of the safe basin, the erosion profile is generated in function of the normalized imposed load. Such a profile enables to measure the imperfection sensitivity of shells and, consequently, to study the influence of different types of imperfections.

4.1. Performance Function

For the buckling analysis of shells subjected to axial compression, a performance function $p_f(X)$ can be expressed as the difference between the buckling load $L_c(X)$ of the shell with imperfections and the applied axial load L_a:

$$p_f(X) = L_c(X) - L_a \qquad (1)$$

where X is the vector of varying control parameters.

The performance function enables for assessing the load-carrying capability of the shell against perturbations, here given by the initial imperfections.

4.2. Control Parameters

The perturbations to the equilibrium state of nominally-perfect shells are taken in the form of two types of initial geometric imperfections: axisymmetric and asymmetric.

The axisymmetric geometric imperfections are characterized by a sinusoidal shape in the axial direction and are modeled by the sine function:

$$w/t = \xi \sin(i\pi z / l_f) \qquad (2)$$

where w is the radial displacement (positive outward); ξ is the magnitude of the imperfections relative to the total thickness t of the shell; l_f is the free length of the shell; and i is the integer denoting the number of axial half-waves.

The asymmetric geometric imperfections are assumed sinusoidal in the axial direction and cosinusoidal in the circumferential direction. They are described using the sine-cosine function:

$$w/t = \xi \sin(i\pi z / l_f) \cos(jy / r) \qquad (3)$$

where i and j are integers denoting the number of axial half-waves and of circumferential waves, respectively.

The control parameters, used in modeling the geometric imperfections, are the imperfection amplitude and the number of axial half-waves for the axisymmetric imperfections, and the number of axial half-waves and of circumferential waves for the asymmetric imperfections.

4.3. Safe Basin

The Cell-to-Cell Mapping Technique [20] is here adapted for the buckling problem of axially-compressed shells.

At first, the control space is delineated in terms of the control parameters, which model the geometric imperfections. It is then discretized in cells of equal size as result of the partition of each control parameter into a number of intervals of uniform size. The control domain is illustrated in Fig. 2 for the two sources of imperfections. The dashed black lines delimit the cells and the dots stand for the center of the corresponding cells.

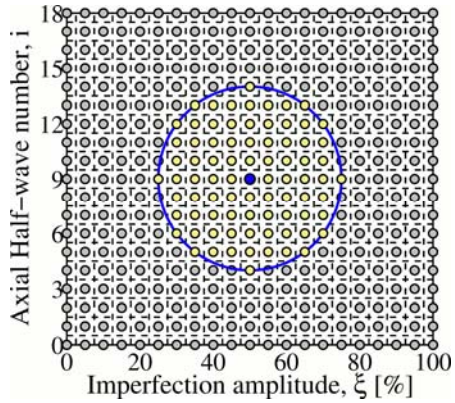

Control domain of axisymmetric imperfections

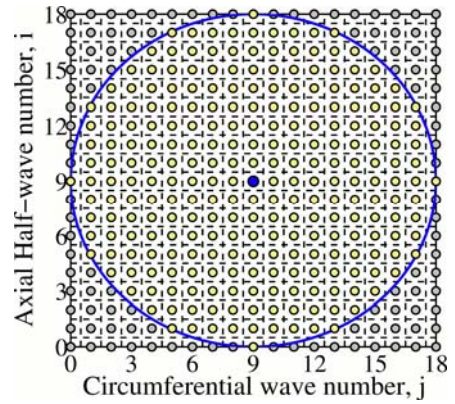

Control domain of asymmetric imperfections

Fig. 2. Control domains.

In the case of perturbations in the form of axisymmetric imperfections, the control domain is delimited by the amplitude to thickness ratio $\xi \in [0\%,100\%]$ and by the number of axial half-waves $i \in [0,18]$. In the case of perturbations in the form of asymmetric imperfections, the control domain is delimited by the number of axial half-waves $i \in [0,18]$ and by the number of circumferential waves $j \in [0,18]$. The amplitude to thickness ratio is set constant and equal to 30% of the total thickness.

Next, explicit dynamic analyses of shell with imperfections are carried out using the finite element code ABAQUS v.6.13 [19] in order to obtain the buckling response over the domain as function of the control parameters and of the axial load.

Finally, the topology of the control space is defined in terms of the performance function for each increment in the applied axial load. In particular, the topology of the basin is arranged in a matrix, which evolves as axial compression increases. The elements of the matrix consist only of two integers at each load level: zero if the shell does not buckle and one if the shell buckles. The elements of the matrix equal to zero delineate the safe basin. The matrix can be graphed as a two-dimensional black and white color-map. The safe basin is identified by white color, whereas the unsafe basin is represented by black color. The unsafe basin expands as the axial compression increases. Consequently, a different color-map of the basin is associated to each load level.

4.4. Integrity Measures and Erosion Profile

The erosion profile of the safe basin is here obtained by plotting two integrity measures [8-9]: the global integrity measure (GIM) and the integrity factor (IF), in function of the increasing applied load.

The global integrity measure takes into account the robustness of the basin and is defined as the hypervolume of the safe basin normalized by a reference value. This measure is calculated as the ratio between the number of pairs of control parameters (ξ, i) or (i, j) for which the shell withstands compression without undergoing buckling divided by the total number of pairs in the control domain.

The integrity factor is a measure of compactness of the basin, and is defined as the normalized radius of the largest hypersphere that entirely belongs to the safe basin. It is a dimensionless measure easy to calculate, like the GIM, and besides enables to eliminate fractal tongues from integrity evaluation. Since

the control space is here two-dimensional, the hypersphere is actually a circle.

To assess the integrity factor, the control domain is discretized in cells; the radius r_c of the largest circle that can be traced into the safe basin is identified, where the radius r_c is expressed in number of consecutive pairs (ξ, i) or (i, j). The number of pairs which are in the circle is calculated, and the integrity factor is assessed as the ratio between this number of pairs and the total number of pairs in the control domain. Fig. 2 illustrates two examples of estimate of the integrity factor. The blue dot stands for the center of the circle of radius r_c. The yellow dots are the pairs inside the circle, whereas the gray dots are the pairs outside the circle. The integrity factor is the ratio between the number of yellow dots and the number of total dots. As a consequence, the integrity factor is a discrete measure.

After having generated the basin of attraction of the fundamental equilibrium state for each increment of the applied axial load, the two integrity measures are assessed at each load level. They are graphed in function of the increasing compressive load, attaining the erosion profile, as shown in Fig. 3. The erosion profile provides a graphical visualization of the reduction, caused by the perturbations, of the load-carrying capability of the axially-compressed shells. The region below the curve is divided into two sub-regions. The gray area denotes the "uneroded basin" sub-region, where the safe basin is not corrupted by perturbations. Such a sub-region extends up to the load level for which the onset of erosion of the safe basin occurs. The blue area identifies the "eroded basin" sub-region and, consequently, it provides an immediate visualization of the degradation of the safe basin.

The magnitude of integrity measure decreases as axial compression increases. The threshold, i.e the load level, for which erosion takes place, depends on the extension of the safe basin. The larger is the safe basin, the larger is the sub-region of "uneroded basin". Consequently, the threshold moves towards right as the width of safe basin increases, i.e. the shell is low sensitive to imperfections.

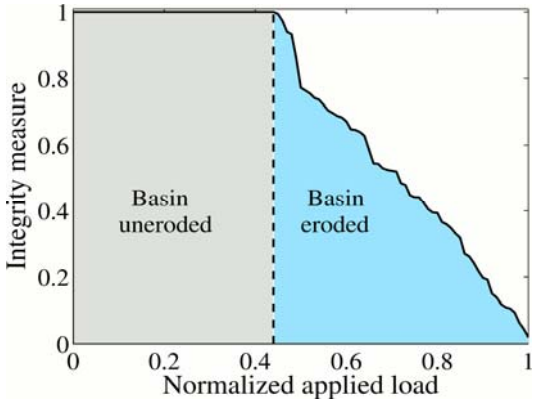

Fig. 3. Erosion profile.

5. Results

The two configurations (SYLDA and SYLDA with cut-outs) of the scaled models of the Dual Launch System of Ariane 5 launcher are studied using the developed approach based on the chaos theory. Two types of geometric imperfections are incorporated in the buckling investigation: axisymmetric and asymmetric.

5.1. Sensitivity to Axisymmetric Geometric Imperfections

The erosion profile of safe basin which surrounds the equilibrium state corresponding to the buckling load of nominally-perfect SYLDA and SYLDA with cut-outs is calculated. The erosion profile measures the sensitive of the two shells to perturbations of the equilibrium in the form of axisymmetric geometric imperfections. Fig. 4 and Fig. 5 show the erosion profile for SYLDA and SYLDA with cut-outs, respectively.

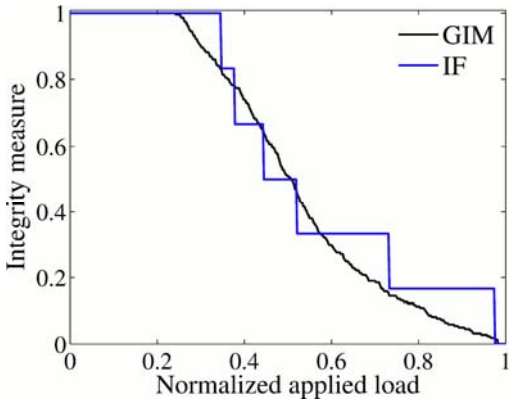

Fig. 4. Erosion profile of SYLDA considering axisymmetric geometric imperfections.

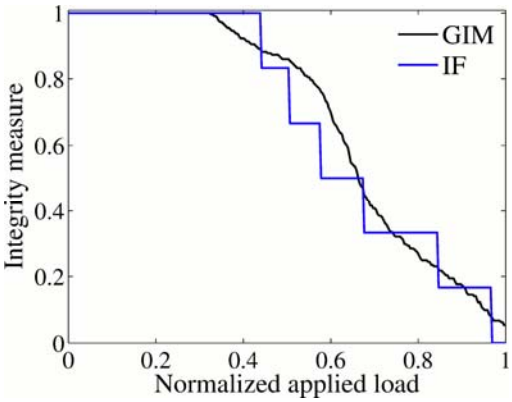

Fig. 5. Erosion profile of SYLDA with cut-outs considering axisymmetric geometric imperfections.

For each shell the erosion profile is attained by graphing both the global integrity measure and the integrity factor as function of the normalized axial load. The normalized axial load is calculated dividing the imposed axial load by the maximum load reached by shell. The maximum load achieved by SYLDA and SYLDA with cut-outs is equal to 417 *kN* and 294 *kN*, respectively [16].

For both the investigated shells, the global integrity measure versus the normalized applied load curve agrees with the integrity factor versus the normalized applied load curve.

Since the erosion of safe basin for SYLDA with cut-outs takes place at a load level higher than for SYLDA, SYLDA with cut-out turns to be less sensitive to axisymmetric geometric imperfections. This outcome is likely due to the presence of cut-outs, which dominate the buckling response of the shell.

An integrity measure equal to 0.20 is assumed to provide an example for the shell design [21]. It means that it is not allowed that the maximum extension of the safe basin decreases below 0.20 of total area. Such a requirement results in calculating the threshold of axial load beyond which the load-carrying capability of the shell is degraded more than 80%. Table 3 lists the load values o for the two shells.

Despite the low sensitivity to axisymmetric geometric imperfections, SYLDA with cut-outs reaches load levels lower than the ones reached by SYLDA for a required integrity measure of 0.20, as a consequence of the presence of the cut-outs.

Integrity measure	Load value for SYLDA	Load value for SYLDA with cut-outs
GIM=0.20	284 *kN*	256 *kN*
IF=0.20	304 *kN*	250 *kN*

Table 3. Load values for axisymmetric imperfections corresponding to integrity measure of 0.20.

The decreasing trend of the two integrity measures, evident in Fig. 4 and Fig. 5, indicates that the safe basin which surrounds the equilibrium configuration corresponding to the buckling load of nominally-perfect shells is eroded by the geometric imperfections. As an example, Fig. 6 shows the topology of the safe basin for SYLDA at two different levels of applied compressive load. It can be observed that the safe basin, represented as white area, shrinks as axial compression increases. In the figure the largest circle of radius r_c, entirely belonging to the safe basin, is also illustrated at each load level.

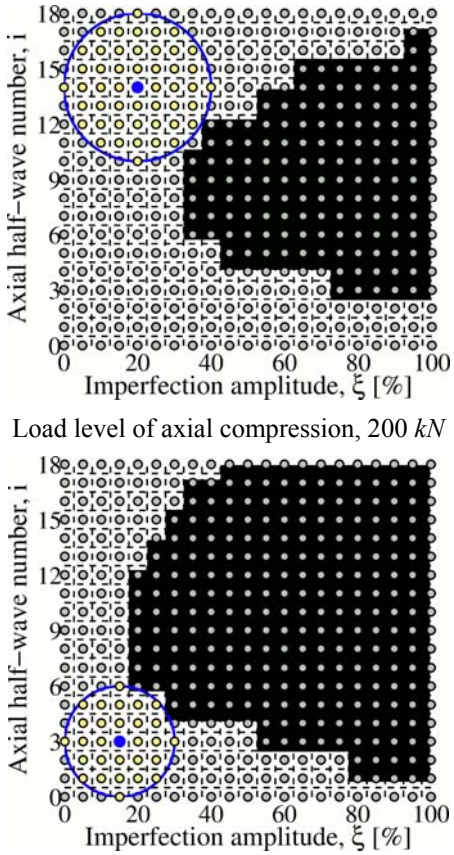

Load level of axial compression, 200 *kN*

Load level of axial compression, 250 *kN*

Fig. 6. Basin surrounding the equilibrium state related to the buckling load of SYLDA.

5.2. Sensitivity to Asymmetric Geometric Imperfections

The erosion profiles of SYLDA and SYLDA with cut-outs in the analysis case of perturbations in the form of asymmetric geometric imperfections are reported in Fig. 7 and Fig. 8, respectively. As in the previous analysis case, the curve resulting from the global integrity measure agrees with the curve resulting from the integrity factor.

Fig. 7 and Fig. 8 show that SYLDA and SYLDA with cut-outs are less sensitive to asymmetric geometric imperfections than to axisymmetric geometric imperfections. Indeed, the onset of the erosion of safe basin occurs for both shells at a higher load level in comparison to Fig. 4 and Fig. 5.

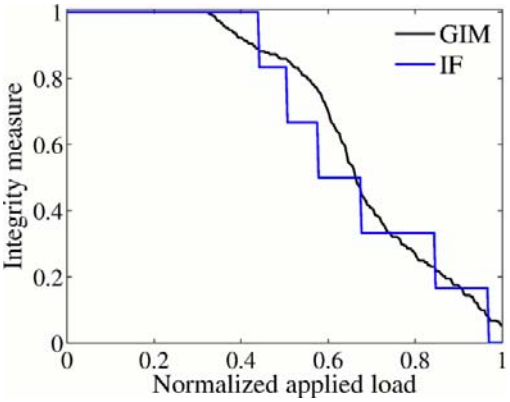

Fig. 7. Erosion profile of SYLDA considering asymmetric geometric imperfections.

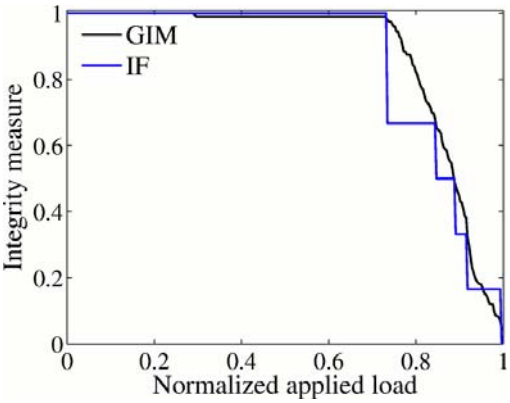

Fig. 8. Erosion profile of SYLDA with cut-outs considering asymmetric geometric imperfections.

In Table 4, the load values related to the erosion profiles for the two shells are summarized for a requirement of integrity measure set to 0.20.

Integrity measure	Load value for SYLDA	Load value for SYLDA with cut-outs
GIM=0.20	346 *kN*	276 *kN*
IF=0.20	338 *kN*	270 *kN*

Table 4. Load values for asymmetric imperfections corresponding to integrity measure of 0.20.

The comparison of the results reported in Table 4 with those of Table 3 points out again that the load-carrying capability of the two considered shells is more affected by the axisymmetric geometric imperfections than by the asymmetric geometric imperfections.

6. Conclusions

A chaos approach for the buckling analysis of composite cylindrical shells under axial compression is developed using the concepts of chaos theory. The approach aims to attain an erosion profile in function of the increasing compressive load. Such a profile is a graphical representation that illustrates the imperfection sensitivity of the shells showing the erosion of the load-carrying capability of the shells due to the geometric imperfections as the axial compression increases.

The chaos approach is applied to the buckling investigation of two configurations of axially-compressed cylindrical shells. The first configuration does not have cut-outs, whereas the second one includes three circular cut-outs. Two types of geometric imperfections are incorporated separately into the analysis: axisymmetric and asymmetric imperfections.

The erosion profile is derived for both shells, showing that the influence of the axisymmetric geometric imperfections is more detrimental than the one of the asymmetric geometric imperfections.

The proposed approach is based on an innovative use of the concepts of chaos theory. The approach can be applied to investigate the imperfection-sensitivity of laminated composite shells and of sandwich composite shells incorporating several types of imperfections.

The approach can be adopted in a preliminary design phase when a test-originated database concerning manufacturing and in-service imperfections is rarely available, in

order to achieve a first assessment of the effects of imperfections on the load-carrying ability of axially-compressed shells.

However, the paper presents only a preliminary study of the chaos theory applied to the buckling analysis of cylindrical shells under axial compression, and the presented methodology needs to be further enhanced. In particular, a best comprehension of the integrity measures is required. Besides, it is important to note that the results are affected by assumed perturbations to equilibrium state and by the specified control domain.

7. References

[1] Koiter WT. *On the stability of elastic equilibrium*. PhD thesis, Delft University of Technology, Delft, Netherlands, 1945. English Translation NASA-TT-F-10833.

[2] *NASA SP-8007-Buckling of thin-walled circular cylinders*. National Aeronautics and Space Administration, Washington, DC, USA, 1968.

[3] Bisagni C. Numerical analysis and experimental correlation of composite shell buckling and post-buckling. *Composites Part B*, Vol. 31, No. 8, pp 655-667, 2000.

[4] Bisagni C and Cordisco P. An experimental investigation into the buckling and postbuckling of CFRP shells under combined axial and torsion loading. *Composite Structures*, Vol. 60, No. 4, pp 391-402, 2003.

[5] Bisagni C. Composite cylindrical shells under static and dynamic axial loading: an experimental campaign. *Progress in Aerospace Sciences*, Vol. 78, 107-115, 2015.

[6] Hilburger MW and Starnes JHJr. Effects of imperfections of the buckling response of composite shells. *Thin-Walled Structures*, Vol. 42, pp 369-397, 2004.

[7] Castro SGP, Zimmermann R, Arbelo MA, Khakimova R, Hilburger MW and Degenhardt R. Geometric imperfections and lower-bound methods used to calculate knock-down factors for axially compressed composite cylindrical shells. *Thin-Walled Structures*, Vol. 74, pp 118-132, 2014.

[8] Thompson JMT and Stewart HB. *Nonlinear dynamics and chaos*. 2nd Edition, John Wiley & Sons, 2001.

[9] El Naschie MS, Al Athel S and Walker AC. Localized buckling as statical homoclinic soliton and spatial complexity. In: *Nonlinear dynamics in engineering systems*, Springer, pp 67-74, 1990.

[10] Gonçalves PB, Silva FMA and Del Prado ZJGN. Global stability analysis of parametrically excited cylindrical shells through the evolution of basin boundaries. *Nonlinear Dynamic*, Vol. 50, pp 121-145, 2007.

[11] Awrejcewicz J and Krysko VA. *Chaos in structural mechanics*. Springer, 2008.

[12] Thompson JMT, Rainey RCT and Soliman MS. Ship stability criteria based on chaotic transients from incursive fractals. *Philosophical Transactions: Physical Sciences and Engineering*, Vol. 332, pp 149-167, 1990.

[13] Soliman MS and Thompson JMT. Integrity measures quantifying the erosion of smooth and fractal basins of attraction. *Journal of Sound and Vibration*, Vol. 135, No. 3, pp 453-475, 1989.

[14] Rega G and Lenci S. Identifying, evaluating, and controlling dynamical integrity measures in non-linear mechanical oscillators. *Nonlinear Analysis: Theory, Methods & Applications*, Vol. 63, No. 5-7, pp 902-914, 2005.

[15] http://www.desicos.eu

[16] Alfano M and Bisagni C. A probabilistic approach for buckling analysis of sandwich composite cylindrical shells. *23rd Conference of the Italian Association of Aeronautics and Astronautics*, Torino, Italy, pp 1-12, 2015.

[17] Bisagni C, Vescovini R and Dávila CG. Single-stringer compression specimen for the assessment of damage tolerance of postbuckled structures. *Journal of Aircraft*, Vol. 48, No. 2, pp 495-502, 2011.

[18] http://www.rohacell.com/sites/dc/Downloadcenter/Evonik/Product/ROHACELL/product-information/ROHACELL%20WF%20Product%20Information.pdf

[19] ABAQUS 6.13 Online Documentation, 2013.

[20] Hsu CS. *Cell-to-cell mapping: a method of global analysis for nonlinear systems*. Springer, 1987.

[21] Lenci S and Rega G. Load carrying capacity of systems within a global safety perspective. Parts I & II. *Journal of Non-Linear Mechanics*, Vol. 46, pp 1232-1239, 2011.

8. Contact Author Email Address

c.bisagni@tudelft.nl

Copyright Statement

The authors confirm that they, and/or their company or organization, hold copyright on all of the original material included in this paper. The authors also confirm that they have obtained permission, from the copyright holder of any third party material included in this paper, to publish it as part of their paper. The authors confirm that they give permission, or have obtained permission from the copyright holder of this paper, for the publication and distribution of this paper as part of the ICAS proceedings or as individual off-prints from the proceedings.